

Quorum percolation in living neural networks

O. COHEN¹, A. KESELMAN¹, E. MOSES¹, M. RODRÍGUEZ MARTÍNEZ¹, J. SORIANO^{1,2} and T. TLUSTY^{1(a)}

¹ *Department of Physics of Complex Systems, Weizmann Institute of Science - Rehovot 76100, Israel*

² *Departament d'ECM. Facultat de Física, Universitat de Barcelona - Av. Diagonal 647, 08028 Barcelona, Spain, EU*

received 2 September 2009; accepted in final form 16 December 2009

published online 22 January 2010

PACS 87.19.L- – Neuroscience

PACS 87.19.11 – Models of single neurons and networks

PACS 64.60.ah – Percolation

Abstract – Cooperative effects in neural networks appear because a neuron fires only if a minimal number $m > 1$ of its inputs are excited. The multiple inputs requirement leads to a percolation model termed *quorum percolation*. The connectivity undergoes a phase transition as m grows, from a network-spanning cluster at low m to a set of disconnected clusters above a critical m . Both numerical simulations and the model reproduce the experimental results well. This allows a robust quantification of biologically relevant quantities such as the average connectivity \bar{k} and the distribution of connections p_k from different neural densities.

Copyright © EPLA, 2010

Large networks generate complex behavior, as is apparent in diverse systems such as computers, society and biology [1]. In particular, the integration of information from several neighbors leads to highly correlated and collaborative activity [2]. In general, the complexity and capacity of the network increases steeply with the degree of inter-connectivity, as does the difficulty to understand these complex networks. Biological neural networks stand out among these as intriguing complex systems [3]. From cultures in a dish [4] all the way to the brain [5], neural networks display a rich repertoire of activity and functionality, which arises from the interplay between hundreds to millions of neurons. In the simplest picture of a spiking neuron, stimuli (inputs) from connected neurons are “integrated” in the target neuron, which fires once a threshold voltage is reached and then propagates the electric signal on to other neurons [6].

Imposing the need for a large quorum of m input nodes to fire leads to a percolation problem, which we term “quorum percolation” (QP). This name also hints for the potential uses of QP to treat the spread of diseases, rumors and opinions. In this work we show how the multiple inputs requirement modifies significantly the function of the network. The QP approach takes the number of inputs required for firing m as its control parameter and can then explain the transition to a *giant m -connected component*

(GmCC), a continuum of connected neurons that fire together and span a significant fraction of the network.

The QP setting is similar to that of bootstrap percolation (BP) in which nodes with less than k neighbors are iteratively “pruned” from a graph until there remains only its highly interconnected “ k -core” ([7–10] and references therein). The propagation of firing in QP is analogous to the advancement of the pruning process in BP (see [10]). In practice, however, physical realizations of BP are usually limited in their connectivity, often on the order of $\bar{k} = 2–3$. In contrast, the average connectivity in the neural network studied here is much higher, $\bar{k} = 50–150$ [11], and results in a very different behavior of the network. A variation on the problem was posed in [12], where the propagation depends on the fraction of ignited neighbors and was solved using the approach presented in [13].

Model. – The neural network is modeled as a random directed graph [14] whose nodes are neurons connected by synapses. The input degree distribution is p_k . Each neuron is assigned a probability $f = f(V)$ to fire in response to the direct excitation by an externally applied electrical voltage. The total probability of a single neuron to fire, Φ , is the sum of $f(V)$ and of its response to the input from the firing of “neighboring” (*i.e.* connected) neurons. This response is characterized by the *collectivity* $\Psi_m(\Phi)$, the probability that there is a quorum of at least m inputs to a neuron that fire and thus excite the neuron. $\Psi_m(\Phi)$ is

^(a)E-mail: tsvi.tlusty@weizmann.ac.il

the synaptic excitation probability, which is the signature of collective effects in the network. Therefore, $\Phi(m, f)$ is given by

$$\begin{aligned}\Phi(m, f) &= f + (1 - f)\Psi_m(\Phi) \\ &= f + (1 - f) \sum_{k=m}^{\infty} p_k \sum_{l=m}^k \binom{k}{l} \Phi^l (1 - \Phi)^{k-l}.\end{aligned}\quad (1)$$

Equation (1) represents the fixed point of an iterative firing process that starts with the external ignition of a fraction $f(V)$ of neurons and propagates by igniting at every step those neurons that accumulated at least m firing inputs. Equation (1) exploits the effective tree-like topology of the random network to ignore the presence of feedback loops and of recurrent activity in the neural culture. The validity of the random graph approximation to metric graphs such as the experimental neural networks is discussed in detail in [10]. It proves convenient to express the collectivity $\Psi_m(\Phi)$ in terms of the generating function $J(z)$ of the degree distribution p_k , $J(z) = \sum_k p_k z^k$, which results in a truncated Taylor expansion $\Psi_m(\Phi) = 1 - \sum_{l=0}^{m-1} (\Phi^l/l!) \partial^l J / \partial z^l|_{z=\Phi}$.

We previously [14] treated a simplified version of equation (1) for the standard bond percolation case of $m = 1$, and observed a percolation transition both in the model and the experiment. The percolated phase is characterized by a giant connected component that spans a non-zero fraction of the network. Note that the GmCC is very different from the conventional $m = 1$ giant connected components.

Here we treat the case of an arbitrary m and find how excitation by multiple inputs changes the response of the neural network. Within the framework of the model, all distributions of connections p_k in the network are possible. However, when coming to compare to particular results in a quantitative manner the need to choose a specific distribution arises. This allows numerical simulations of the model and a comparison to data from the experiment. The optimal choice was determined previously [11,14] to be a Gaussian, based on numerical simulation comparing data from experiment —both the giant component size g [11] and the cluster size distribution p_s [14]. After trying a variety of distribution functions (including the natural candidates, *i.e.* power laws, exponential and Poisson), we concluded that the Gaussian distribution gave the best description.

Following the experiment, we specify the degree distribution p_k and solve for $\Phi(m, f)$ as a function of m and f , the experimental control parameters. Based on our previous experimental observations [11,14], we assume a Gaussian distribution $p_k \sim \exp[-(k - \bar{k})^2 / (2\sigma^2)]$ with $\bar{k} = 50$ and $\sigma = 15$.

To find the firing probability $\Phi(m, f)$ for given values of m and f , we rearrange equation (1) as $f(m, \Phi) = (\Phi - \Psi_m(\Phi)) / (1 - \Psi_m(\Phi))$. In fig. 1(a), $f(m, \Phi)$ is plotted and graphically inverted to find the solution $\Phi(m, f)$.

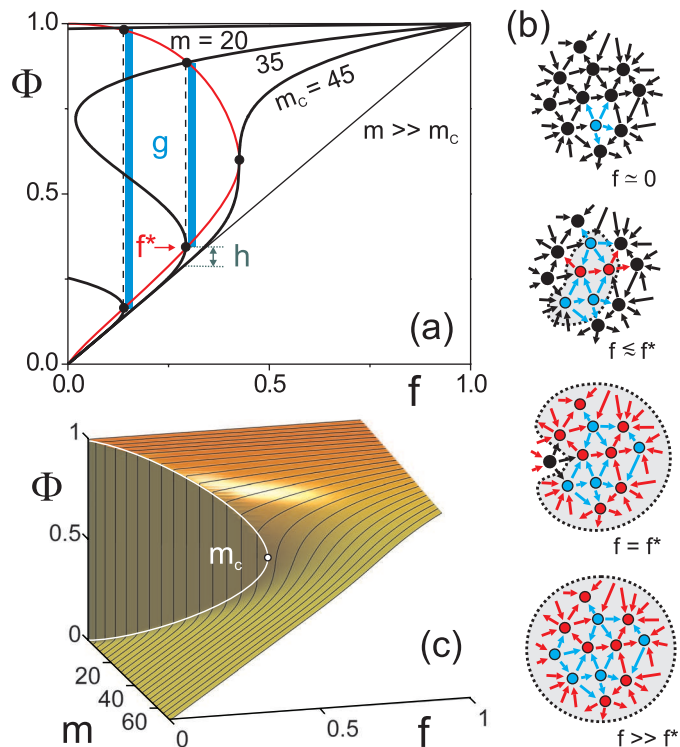


Fig. 1: (Colour on-line) Quorum percolation model. (a) Black lines: Family of solutions $\Phi(m, f)$ for increasing m and a Gaussian degree distribution p_k with $\bar{k} = 50$ and $\sigma = 15$. Dashed lines connect the physical solutions in the coexistence region. The jump in Φ for each value of f^* identifies g , the size of the GmCC (blue bars), and the contribution of the small clusters h . For example, for $m = 20$ at $f = 0$ Φ grows continuously from zero, so that at $f = 0$ there is no GmCC. Although the upper branch exists at lower values for $m = 20$, the GmCC appears only at $f \approx 0.15$, and Φ then jumps practically to 1. While the clusters comprising h are isolated, the GmCC was observed in the simulations to be connected. The black dots and the red line indicate the transition points $f^*(m)$ and m_c , respectively. (b) Schematic representation of the ignition of the network as a function of f , for a network with $\bar{k} = 5$ and input threshold $m = 3$. Ignition occurs in two phases: first the external ignition of a fraction f of neurons and in the second, the expansion of the firing m -connected cluster (GmCC). For $f \approx 0$ only the neurons (circles) with the lowest excitation threshold are ignited (blue) and pass the signal (blue arrows). As f increases more neurons get excited. These neurons, in turn, excite synaptically other neurons (red), but the activity is confined to isolated clusters. At $f = f^*$ enough neurons fire for the network to percolate and a GmCC emerges. Weakly connected neurons and with high firing thresholds will fire only at large f . The outlined areas show the neurons that fired together for each f . (c) Three-dimensional representation of the solutions of the model as a function of m and f . The white curve shows the values of the transition points f^* .

The solution shows that both parameters f and m have transition values, $f^*(m)$ and m_c , where the solution changes qualitatively. For $m < m_c$, the curve $\Phi(m, f)$ is non-monotonic and below the transition, $f < f^*(m)$, there

exist three solutions: The lower one corresponds to $\Phi \simeq f$ and represents a system where only the externally excited neurons fire. In this solution the external voltage V is only able to ignite “sensitive” neurons, *i.e.* neurons with a low excitation threshold. After they fire, the signal dies out without propagating throughout the network. The second, intermediate solution lies in a non-physical region in which the firing probability decreases with the external electrical stimulus f , *i.e.* $d\Phi/df < 0$. The third, higher solution corresponds to the synaptic excitation of most of the neurons. This solution signals the ignition of the giant connected component of the network. The two available physical solutions, the unexcited network $\Phi(f) \simeq f$ and the excited network $\Phi(f) \simeq 1$ coexist below $f^*(m)$.

The first two solutions merge and disappear at $f = f^*(m)$ (fig. 1(a)) and for $f > f^*(m)$ only the third solution is available. Physically, at this point the external voltage is high enough to excite the GmCC and the whole network percolates. As a precursor to the transition, $\Phi(f)$ deviates from the expected $\Phi(f) \simeq f$. This deviation signals the ignition of small clusters h that contain the most excitable neurons. At this critical value $f^*(m)$ the system undergoes a phase transition, from the low-excitation state characterized by $\Phi \simeq f$ to the percolation solution $\Phi \simeq 1$ where almost all neurons fire (fig. 1(b)). The behavior of the network can be seen as a first-order phase transition that exhibits a discontinuity in the value of Φ . Note that, in contrast to the traditional $m = 1$ percolation, for $m > 1$ the GmCC does not appear at zero excitation. This is because the requirement of multiple inputs imposes a minimal excitation $f^*(m)$, or threshold voltage, to excite the GmCC, which may “immunize” the neural network against excitation by low noise.

The size g of the GmCC decreases as m grows, and reaches $g = 0$ at a critical value $m = m_c$. For $m > m_c$ the demand for multiple inputs is so restrictive that the network has no giant connected component. The network breaks off into isolated clusters that are ignited independently. Graphically, at $f = f^*(m_c)$ the two physical solutions (as well as the unphysical third one) merge into one (fig. 1(a)), and for higher values of both f and m only one solution exists. This scenario corresponds to a second-order phase transition, characterized by the order parameter g , with $g = 0$ for $m > m_c$ and $g > 0$ for $m \leq m_c$. At the extreme of $m \gg m_c$ the network is completely disconnected, neurons are ignited in response to the external excitation only, and the solution $\Phi \simeq f$ applies for all values of f .

The non-monotonic curve of $\Phi(f)$ is similar to the van der Waals density-pressure isotherms, which exhibit a gas-liquid coexistence region below a critical temperature (equivalent to m_c). The non-physical segment of the isotherm is resolved by Maxwell’s construction which connects the coexisting phases by a vertical line, signifying a first-order phase transition. In a similar way, we replace the coexistence region of the $\Phi(f)$ curves by a vertical line, connecting the two physical solutions of the system

(dashed lines in fig. 1(a)). This line identifies the size g of the GmCC. In contrast to the traditional liquid-gas transition which occurs at around the center of the coexistence region, our simulations show that ignition of the GmCC occurs very close to f^* .

Figure 1(c) summarizes the response of the network as a function of Φ , m and f . The white curve shows $f^*(m)$, and identifies the first-order phase transition in the size of the GmCC. This curve disappears at $m = m_c$, where the network undergoes a second-order, continuous phase transition. The point $m = m_c$ is analogous to the classical tricritical point of thermodynamic phase transitions.

Experiment. – The ideas of QP are tested on a typical two-dimensional *in vitro* culture comprising of over 5×10^5 neurons. The experimental system (see refs. [11,14,15] for details) is a culture of neurons that are extracted from rat embryonic brains in day 17 or 19 of pregnancy. Neurons are plated on a glass coverslip and create a highly connected two-dimensional network in about 2 weeks. Activity can be stimulated globally in the culture by an external voltage V that is applied across two bath electrodes.

We assume that a neuron integrates over its input connections, has a threshold voltage V_T to be ignited, and that on average each input into a neuron contributes a voltage g_{syn} . Thus, $m_0 = V_T/g_{\text{syn}}$ inputs are initially required to excite a neuron and propagate the signal in the network. The synaptic strength can be reduced by application of a blocker 6-cyano-7-nitroquinoxaline-2,3-dione (CNQX) for the synaptic α -amino-3-hydroxyl-5-methyl-4-isoxazole-propionate (AMPA) glutamate receptor. Administering CNQX in increasing concentration gradually decreases the synaptic bond between neurons, and thus increases the number of inputs m needed for a neuron to fire. The relation between the input threshold m and the concentration of CNQX is given by $m = m_0(1 + [\text{CNQX}]/K_d)$ [11], with $K_d = 300$ nM. We use $m_0 \simeq 15$ as the the initial input threshold for the unperturbed network [11].

Signals in the neural network are transferred within the cells by an electric action potential, and between cells by chemicals that are detected by specific receptors at the synapses. The major types of receptor that a neuron has are receptors of type AMPA and NMDA (N-methyl-D-aspartic acid) for the excitatory neurotransmitter glutamate, and receptors for the inhibitory neurotransmitter GABA_A (γ -Aminobutyric acid). In the experiments reported here the NMDA and GABA_A receptors were completely blocked by their antagonists (2R)-amino-5-phosphonovaleric acid (APV) and bicuculline, respectively, leaving AMPA as the dominant receptor. Thus inhibition is practically turned off, and we measure a network that is uniquely excitatory.

CNQX is a highly specific antagonist of the AMPA receptors, with little or no effect on other receptors. Its effect is to block AMPA receptors and thus reduce the synaptic strength. This does not directly affect

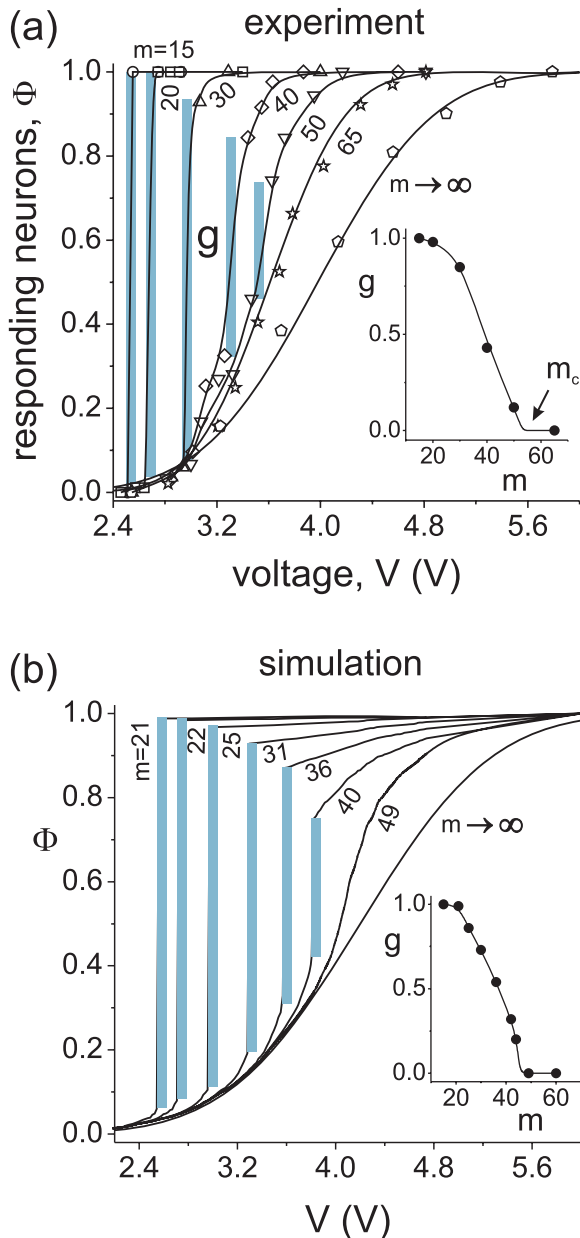


Fig. 2: (Colour on-line) (a) Experimental $\Phi(V)$ curves for gradually higher concentrations of CNQX, between 0 and $10\ \mu\text{M}$, and with $m = m_0(1 + [\text{CNQX}]/K_d)$, where $K_d = 300\ \text{nM}$ and $m_0 = 15$. (b) $\Phi(V)$ curves from a numerical simulation of the model with a Gaussian p_k , $\bar{k} = 40$ and $\sigma = 20$. Vertical bars show the size of the GmCC g . The insets show the corresponding size of the GmCC as a function of m . For the experiments, the values of g are averaged over two consecutive $\Phi(V, m)$ explorations of the network. Lines are a guide to the eye.

the network architecture, in the sense that it does not change any hardwired connection (although of course, for sufficiently high concentrations the synapses are totally blocked, and at that final stage the network topology does change).

If inhibition is not neutralized by bicuculline, then the balance of excitatory and inhibitory neurons is crucial for the behavior of the network. In the framework of our

simplified model, it suffices to approximate the contribution of inhibitory synapses by a simple negative voltage input (subtraction) to the membrane potential. This is based on known values of the post synaptic current in both excitatory and inhibitory synapses, which are similar [11,16].

For a given network with a probability distribution of input connections p_k , the pair of control parameters (m, V) completely determines the firing of the network. Initially, for the unperturbed network, $m = m_0$ is much smaller than the average connectivity of the neurons $\bar{k} = \sum_k k p_k$ [11]. Hence, a small fraction of firing neurons can ignite all the rest and Φ jumps abruptly to 1, so that the GmCC comprises almost all the network (fig. 2(a)). As CNQX is added, the connectivity decreases and m grows. Those neurons having less than m inputs get disconnected from the network and, in turn, reduce the number of inputs of their target neurons. The fraction Φ of neurons that respond together to a given voltage V reduces in size. The biggest jump in Φ , which identifies the size g of the GmCC, gradually decreases. At a critical value $m = m_c$, the GmCC disintegrates into isolated m -connected clusters. When the network is fully disconnected then the neurons respond only to the external excitation. The value of m_c is a reliable and reproducible experimental measurement, and forms the basis for evaluating several biologically relevant measures of the connectivity in a neural culture [11,16]. A possibility which is ignored here but can be accommodated in the model is that m is a function of V .

Simulations. – A random, directed graph was created by assigning to each vertex a number of in- and out-edges, according to the given Gaussian distribution. The total numbers of in and out edges were equated by randomly removing or adding out-edges. Connections were made by iteratively connecting the pair of nodes with the highest number of available out- and in-edges. The resulting graph was randomized by switching vertices between randomly selected pairs of edges.

Each vertex was also assigned a random sensitivity f to the external voltage V , drawn from a Gaussian distribution, which was later fit to the experimentally measured sensitivity of the neurons in the culture. The parameters determining each simulation were m and the external voltage V . In a typical run m was increased from 2 to 50, and V was varied from V_{\min} to V_{\max} so that $f(V_{\min}) \simeq 0$ and $f(V_{\max}) \simeq 1$. At each V those neurons with $f(V) > 0$ were first ignited, which in turn excited connected neurons that satisfied the input threshold requirement. The total fraction of nodes firing $\Phi(m, V)$ was stored for further analysis. An increase of more than 10% in the firing response of the network at a single step was considered to be the signature of the GmCC $g(m)$. We also extracted $f^*(m)$ for each run. All values were averaged over 10–50 different realizations of random graphs created with the same parameters.

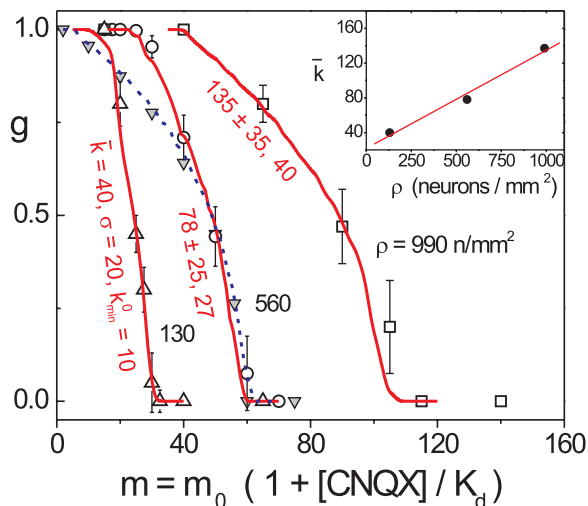


Fig. 3: (Colour on-line) Main plot: Experimental $g(m)$ curves for 3 different neuronal densities (open symbols, each data set averaged over 4 experiments) are fitted to numerical simulations of the model for p_k Gaussian (red, each curve averaged over 5 realizations). The values in red indicate the parameters of the simulations: \bar{k} , σ and the outer cutoff k_{\min}^o . In all cases $k_{\min}^i = k_{\min}^o$. The grey triangles show the numerical integration of the model for $\bar{k} = 78$ and $\sigma = 25$, compared to numerical simulations with the same parameters and for $k_{\min}^i = 27$, $k_{\min}^o = 0$ (blue dashed line, average over 10 realizations). Inset: average connectivity \bar{k} (extracted from the simulations) as a function of the density ρ of the neural culture.

Comparison of simulation and experiment. – Figure 2 shows the comparison of a particular realization in the simulation to a single experimental run. Both experiment and a single simulation include fluctuations in the choice of the connections, and are therefore noisy. This leads to some discrepancies in the quantitative agreement of the simulation with the experiment, for example for $m = 49$ in the model $g = 0$ while in the experiments it is still non-zero at $m = 50$. Furthermore, measuring average quantities means that we may be describing only the majority of the population, while some small fraction of the neurons, too small to disrupt the average properties, may obey statistics that deviate from the Gaussian distribution. Still, in both cases a finite f is needed to induce the transition to a GmCC, and the emergence of a critical m_c occurs in a similar way. The inset shows a detail of the development of the GmCC as a function of the input threshold m .

A particularly relevant comparison of experimental and simulation results is obtained as the experimental densities of neurons is varied. The effect of increasing the density is to increase the average connectivity \bar{k} that characterizes the distribution p_k [11]. Figure 3 shows the measured transition curves of g as function of m at different densities. The curves are characterized by the presence of a plateau $g(m) \simeq 1$ for low values of m . The GmCC gradually decreases for higher m , and disappears at the transition point m_c .

In the simulations, the distribution p_k has to be varied in order to follow the experimental behavior. The connectivity is described by Gaussians with increasing \bar{k} and σ . To reproduce the experimental plateau, however, a cutoff $k_{\min}^{i,o}$ in both the input i and output o degree distributions has to be applied, so that $p_k^{i,o} = 0$ for $k^{i,o} < k_{\min}^{i,o}$. Overall, as seen by the red lines in fig. 3, the agreement of simulation and experiment is striking, and the variation of m_c is exactly reproduced. More important, as the inset shows, the change in experimental neuronal densities is linearly related to the changes in average connectivity of the simulation.

Comparison of simulation and model. – The model and simulation fit very well when using the Gaussian distribution of the connections. In a way, this is both encouraging and surprising, since the simulations carry a large number of loops (the number of directed triangles can be estimated by $k^3/6 \sim 8 \times 10^4$), while the model assumes no loops.

The only sign of a deviation of model and simulation appears when we introduce the lower cutoff in the distribution of both the input and output connectivity. This was crucial for reproducing the plateau that characterized $g(m)$ for low m in the experiment. If the cutoff was applied either to only the input or only to the output distribution then the numerical simulations did not give this plateau (dashed line in fig. 3). As for the model, the cutoff in the input distribution (the model disregards the output distribution) had practically no effect on the response of the network (grey triangles in fig. 3).

Discussion. – The existence of a “threshold”, or the demand for a “quorum” of inputs lies at the heart of Integrate and Fire models of the neuron [17], and is basically what allows for computation in neuronal ensembles [18]. Similar mechanisms may be at work in diverse systems such as the creation of public opinion, in which people hear many views before they make their mind up [19], and where f would be construed as external forcing such as the effect of the media. We believe that the QP model supplies a quantitative framework in which to study such processes. In this system, the demand for “more” neuronal inputs leads to a “different” transition and to a more complex threshold behavior [18].

The major departure of the QP from standard percolation is in the ignition process. The need for a significant fraction f^* of the network to be initially activated, and the dependence of f^* on m , is a unique characteristic of the system. We believe that the deviation of the simulated and experimental results from the tree-like model occurs due to the existence of loops, which would be important exactly in the region of small excitations that lead to ignition of the whole network. Many loops accelerate the propagation of the firing cluster and thus the initial fraction f^* may decrease even to zero [10]. The possibility of incorporating inhibitory neurons directly in the model would

also be interesting. We furthermore expect that studies of the behavior of $f^*(m)$ and of m_c for different degree distributions will yield a rich variety of phenomena.

We are grateful to J.-P. ECKMANN for fruitful discussions and insight. This work was supported by the Israel Science Foundation grant No. 1320/09 and by the Minerva Foundation (Munich, Germany).

REFERENCES

- [1] ALBERT R. and BARABASI A.-L., *Rev. Mod. Phys.*, **74** (2002) 47.
- [2] ANDERSON P. W., *Science*, **177** (1972) 393.
- [3] KOCH C. and LAURENT G., *Science*, **284** (1999) 96.
- [4] WAGENAAR D. A., PINE J. and POTTER S. M., *BMC Neurosci.*, **7** (2006) 11.
- [5] SALINAS E. and SEJNOWSKI T. J., *Nat. Rev. Neurosci.*, **2** (2001) 539.
- [6] OSAN R. and ERMENTROUT B., *Physica D*, **163** (2002) 217.
- [7] ADLER J., *Physica A*, **171** (1991) 453.
- [8] BOLLOBAS B. (Editor), *Graph Theory and Combinatorics: Proceedings of the Cambridge Combinatorial Conference in Honor of Paul Erdos* (Academic Press, London) 1984, pp. 35–57.
- [9] PITTEL B., SPENCER J. and WORMALD N., *J. Comb. Theory, Ser. B*, **67** (1996) 111.
- [10] TLUSTY T. and ECKMANN J.-P., *J. Phys. A*, **42** (2009) 205004.
- [11] SORIANO J. *et al.*, *Proc. Natl. Acad. Sci. U.S.A.*, **105** (2008) 13758.
- [12] WATTS D. E., *Proc. Natl. Acad. Sci. U.S.A.*, **99** (2002) 57661.
- [13] CALLAWAY D. S. *et al.*, *Phys. Rev. Lett.*, **85** (2000) 5468.
- [14] BRESKIN I. *et al.*, *Phys. Rev. Lett.*, **97** (2006) 188102.
- [15] ECKMANN J.-P. *et al.*, *Phys. Rep.*, **449** (2007) 54.
- [16] JACOBI S. *et al.*, *Eur. J Neurosci.*, **30** (2009) 998.
- [17] KOCH C., *Biophysics of Computation* (Oxford University Press, New York) 1999.
- [18] FEINERMAN O., ROTEM A. and MOSES E., *Nat. Phys.*, **4** (2008) 967.
- [19] SHAO J., HAVLIN S. and STANLEY H. E., *Phys. Rev. Lett.*, **103** (2009) 018701.